

Dynamics of dark energy and scalar field models in non-flat universe

Iqra Nawazish¹, Wajiha Javed^{2,3}  and Nimra Irshad²

¹COMSATS University Islamabad, Lahore Campus, Pakistan

²Division of Science and Technology, University of Education, Township Campus, Lahore-54590, Pakistan

E-mail: iqranawazish07@gmail.com, wajiha.javed@ue.edu.pk, wajihajaved84@yahoo.com and nimrairshad38@gmail.com

Received 9 October 2019, revised 23 December 2019

Accepted for publication 3 January 2020

Published 18 February 2020



CrossMark

Abstract

This Paper is devoted to study the effects of different scalar field models under the influence of interacting generalized ghost pilgrim dark energy model in the framework of non-flat FRW universe. For this purpose, we examine the behavior of equation of state and Hubble parameters for two different values of interaction term. Moreover, we consider Lagrangian density of quintessence, tachyon, k-essence and dilaton models to check the consistency of dark energy model with scalar field models. We also evaluate their corresponding potentials and discuss the behavior of kinetic as well as potential energies graphically. We also check the consistency of fractional density of matter and dark energy with Planks 2018.

Keywords: dark energy model, scalar field models, non-flat universe

(Some figures may appear in colour only in the online journal)

1. Introduction

The observations from different experiments like Supernovae type Ia [1], cosmic microwave background radiation [2] and large scale structure [3, 4] show that the Universe is in the phase of accelerated expansion. The studies of standard cosmology, based on general relativity (GR), show that the dark energy (DE) is the cause of this rapid expansion [5]. Various models have been presented to know its nature and in order to search the best DE candidate [6–10]. The universe is filled with perfect fluid and some specific ranges of equation of state (EoS) parameter ω , discuss the current stage of universe.

The holographic DE (HDE) is the DE model in the background of quantum gravity having the energy density of the form

$$\rho_{\Lambda} = \frac{3m^2}{8\pi GL^2},$$

here m is constant and L is infrared cut off which is used to explain the size of universe [11, 12]. Further, Wei proposed a new DE model, named as Pilgrim DE (PDE) but it leads toward the violation of cosmic censorship hypothesis [13]. The PDE

model is introduced in order to avoid the formation of black holes. Its energy density is defined as $\rho_{\Lambda} = 3\alpha^2 M_p^{4-\eta} L^{-\eta}$, where L is the length, M_p defines Plank's mass, α and η are dimensionless constants [14]. This model leads to the Phantom dark energy era that avoids the formation of black holes.

A new dynamical model is introduced to examine the current stage of universe now a days, known as ghost DE (GDE) model having energy density $\rho_{\Lambda} = \alpha H$, here α is the constant with dimension of energy. The generalization of GDE upto the second order term of Hubble parameter H is known as generalized GDE (GGDE) model derived by Cai *et al* [15, 16]. Its energy density is given as $\rho_{\Lambda} = \alpha H + \beta H^2$, where β defines the constant having dimension of energy. This DE model plays an important role to explore the dynamics of early universe. While, the incorporation of PDE and GGDE models yield the GGPDE model. The mathematical form of GGPDE model is given as

$$\rho_{\Lambda} = (\alpha H + \beta H^2)^{\gamma},$$

where γ elaborates the pilgrim parameter to analyze the various possibilities for the resistance of the formation of black holes and hence in this background it is really very important to discuss the issue of singularity.

³ Author to whom any correspondence should be addressed.

There are two approaches to deal with the cosmic acceleration currently. One is to establish the scalar field of matter in GR such as tachyon [17], K-essence [18], phantom [19], dilaton [20] and Chaplygin gas etc. Other is the modification of Einstein–Hilbert action to obtain the other theories of gravity like $f(R)$, $f(T)$ and Gauss–Bonnet gravity. The scalar field is the field which occur naturally in particle physics like string theory. For instance, the quintessence scalar field model [21–24], which convincingly discuss the recent days cosmic acceleration by utilizing the late-time attractor solutions.

In recent decades, the compatibility between the DE models with scalar field DE are very daring subject in cosmological phenomenon. Many authors have examined the DE models and cosmological phenomenon [25–30]. Motivated by these work, several authors have analyzed the GGPDE model till now [31, 32].

Inflation models established on the basis of scalar field models, they play a remarkable role in the higher energy physics. In inflationary models with scalar fields, the equation of motion is comprehensible as it is considered that the scalar field is the only matter field found in the early universe. Initially, in GR, it has been clear that the theory admits singular solutions. Matter field, i.e. scalar field can alter the understanding of singularities, it is a major part of research in the field of GR.

At observational scale, there are some proves that the idea of interaction between DE and dark matter (DM) or cold DM (CDM) [33]. The interaction between the DM and energy density is explained by the equation of continuity, where d^2 serves as the interaction parameter between CDM and DE. Granda and Oliveros [34] constructed HDE with scalar field model in flat FRW universe [35]. Karami and Fehri [36] gave the generalization of this work for the non-flat universe. Sheykhi [37] have formulated the quintessence, tachyon, K-essence and dilatonic scalar field models in flat universe.

Jawad *et al* [31] investigated the GGPDE model with scalar field models such as quintessence, tachyon, K-essence and dilaton models for flat FRW universe. They analyzed the dynamics of scalar field models with corresponding potential in the presence of interacting parameter d^2 . For quintessence model, the $\phi(z)$ decreases and $V(\phi)$ increases with the passage of time. For tachyon model, the $V(\phi)$ decreases and $\phi(z)$ increases as universe expand, while for K-essence scalar field model $\phi(z)$, $V(\phi)$ and χ increases as z increases. Also, EoS parameter showed the accelerated expansion.

Sharif and Jawad [38] examined the HDE and scalar field models in the non-flat FRW universe. They studied the interacting NHDE with tachyon, K-essence, quintessence and dilaton scalar field models. They evaluated the potential and dynamics of scalar field models by different values of constant parameter. Inspired by the above work, we analyze the both interacting and non-interacting GGPDE model in the background of non-flat FRW universe for two different values of interaction term. Also, we check the correspondence of DE model with scalar field dark energy models like quintessence, tachyon, dilaton and K-essence. The Paper is outlined as: section 2 contains the first field equation, equation of continuity, derivative of Hubble parameter and EoS. The

section 3 is based on the scalar field models and their graphical analysis. The final remarks are given in the last section.

2. Dynamics of GGPDE model

In this section, we discuss the Hubble parameter and EoS parameter for interacting GGPDE model in non-flat FRW universe

$$ds^2 = -dt^2 + a^2(t) \left(\frac{dr^2}{1 - \kappa r^2} + r^2 d\theta^2 + r^2 \sin^2 \theta d\phi^2 \right). \tag{2.1}$$

Here $a(t)$ is the scale factor and κ is the spatial curvature, where $\kappa = -1, 0, 1$ indicates open, flat and closed universe respectively. In this scenario, the first Friedmann equation takes the form

$$H^2 + \frac{\kappa}{a^2} = \frac{1}{3m^2} (\varrho_m + \varrho_\Lambda), \tag{2.2}$$

where ϱ_m and ϱ_Λ are DM and DE densities respectively. H denotes the Hubble parameter given by $H = \frac{\dot{a}}{a}$, dot is the derivative with respect to t . Rewrite equation (2.2) in terms of fractional density as

$$\Omega_m + \Omega_\Lambda = 1 + \Omega_\kappa, \tag{2.3}$$

where

$$\Omega_m = \frac{\varrho_m}{3H^2}, \Omega_\Lambda = \frac{\varrho_\Lambda}{3H^2}, \Omega_\kappa = \frac{\varrho_\kappa}{3H^2}.$$

we would assume the GGPDE density as follows

$$\varrho_\Lambda = (\alpha H + \beta H^2)^\gamma, \tag{2.4}$$

where γ is the GGPDE constant. The equation of continuity by the interaction between DM and GGPDE becomes

$$\dot{\varrho}_m + 3H\varrho_m = \Upsilon, \tag{2.5}$$

$$\dot{\varrho}_\Lambda + 3H\varrho_\Lambda(1 + \omega_\Lambda) = -\Upsilon. \tag{2.6}$$

We consider the two interaction terms as

$$\Upsilon_1 = 3d^2 H \varrho_{m1}, \tag{2.7}$$

$$\Upsilon_2 = 3d^2 H (\varrho_{m2} + \varrho_\Lambda), \tag{2.8}$$

where d^2 is known as the interacting constant. Using equations (2.5) and (2.7), we get the density of DM as

$$\varrho_{m1} = \varrho_{m0} a^{3(d^2-1)}, \tag{2.9}$$

here ϱ_{m0} is the constant of integration. Similarly, Using equations (2.5) and (2.8), we get the density of DM as

$$\varrho_{m2} = \frac{1}{2} \left(\frac{d^2 \left(\frac{-\alpha^2}{\beta} \right) (2 + \gamma + \gamma^2) + c_1}{d^2 - 1} \right) e^{\frac{-3\alpha(d^2-1)z}{b}}, \tag{2.10}$$

here c_1 is the constant of integration.

We plot the fractional densities of matter and DE against z for three different values of interacting parameter $d^2 = 0.02, 0.0$ and 0.5 for $k = 1, k = -1$ and when Hubble parameter is constant in figures 1 and 2 respectively. The Ω_{m1} is the matter

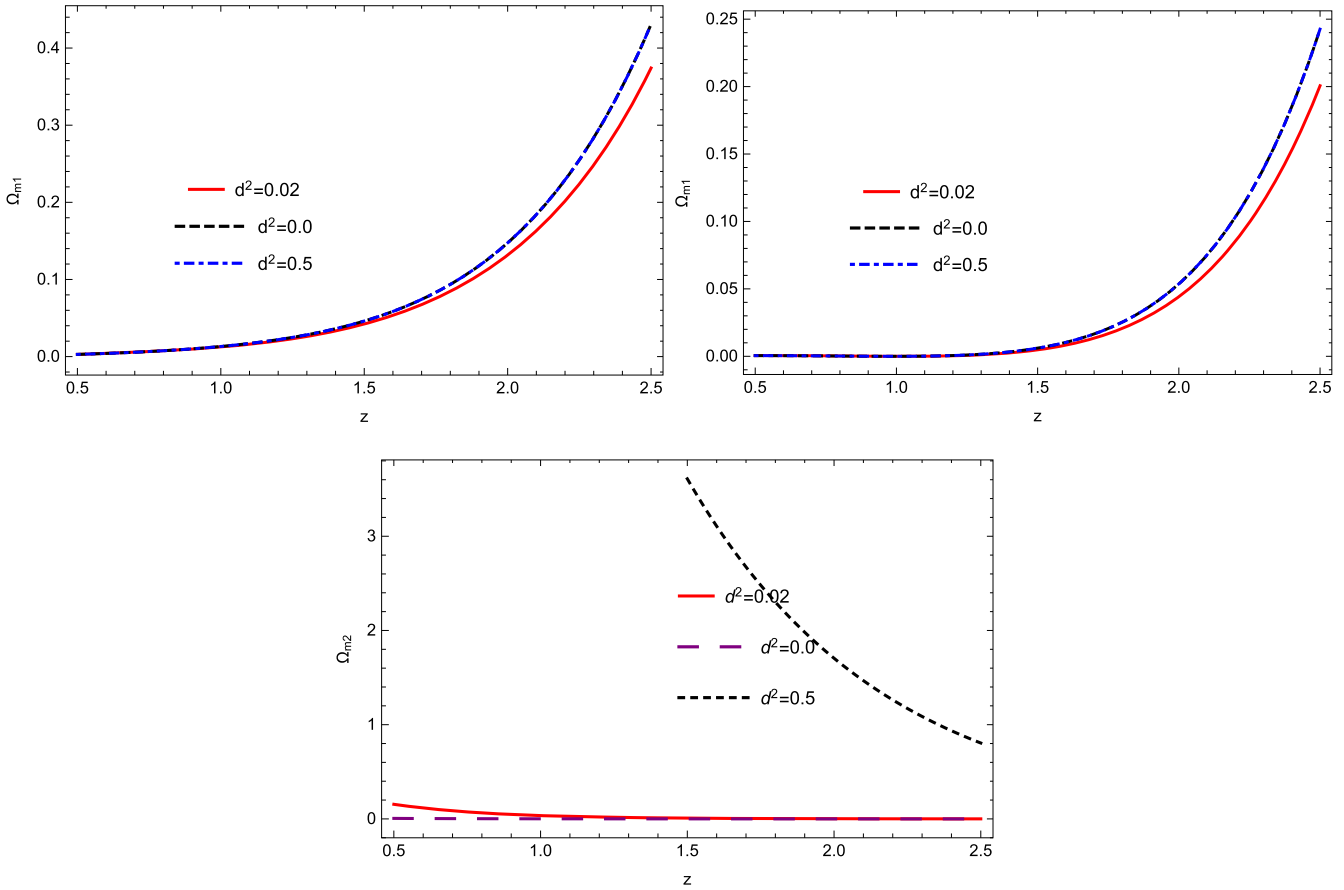


Figure 1. Plot of Ω_{m1} (for $k = 1$ and $k = -1$) and Ω_{m2} versus z .

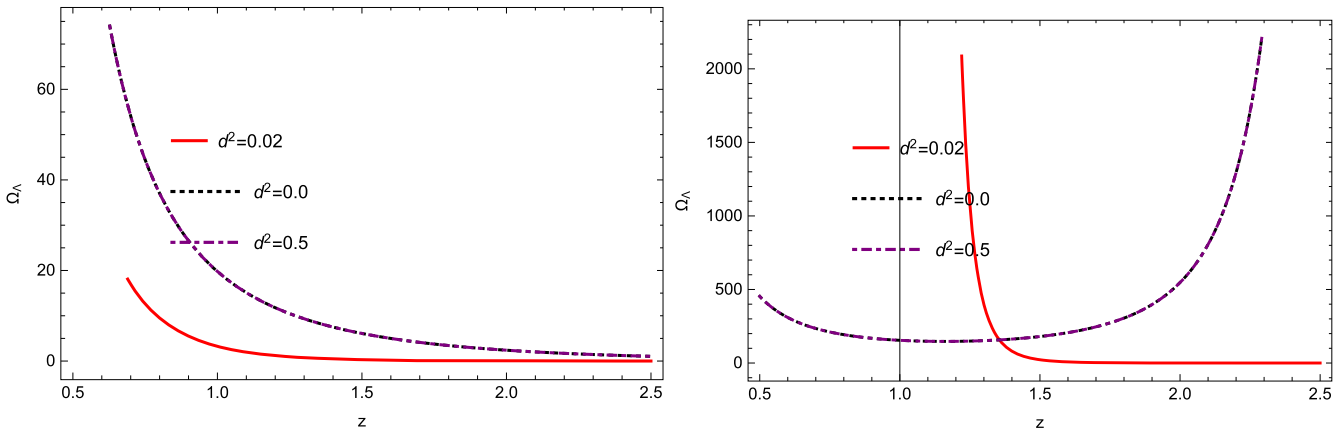


Figure 2. Plot of Ω_Λ (for $k = 1$ and $k = -1$) versus z .

density which is according to ϱ_{m1} whereas, the Ω_{m2} is according to the ϱ_{m2} . There are some recent researches in favor of open and closed universe models with fractional densities according to recent Planck’s 2018 data. It is indicated that $\Omega_m \simeq 0.3111$ and $\Omega_\Lambda \simeq 0.6889$ from the observations of Planck 2018. For $k = 1$, the trajectories of fractional density of matter exhibits $\Omega_m \simeq 0.1111$ which is very closed to data mentioned by Planck 2018 as shown in figure 1. For $k = -1$, the plot of Ω_{m1} does not show consistent behavior with recent data as it shows very small value in accordance with Planck 2018. Similarly, the trajectories of Ω_{m2} exhibits inconsistent

behavior as in figure 1. In figure 2, the trajectories of DE fractional density exhibits $\Omega_\Lambda = 0.6$ implying consistent behavior with Planck 2018 for $k = 1$. For $k = -1$, the plot shows inconsistent behavior with recent observational data as the DE fractional density gains very large value.

Inserting equations (2.4) and (2.9) in (2.2), we obtain differential form of Hubble parameter as follows

$$H'(z) = (3H_0^2\Omega_{m0}(d^2 - 1)a^{3(d^2-1)} - 2\kappa a^{-2}) \times (2(\alpha + \beta H) - \gamma\Omega_\Lambda(\alpha + 2\beta H)(\alpha + \beta H)^{-1})^{-1}. \tag{2.11}$$

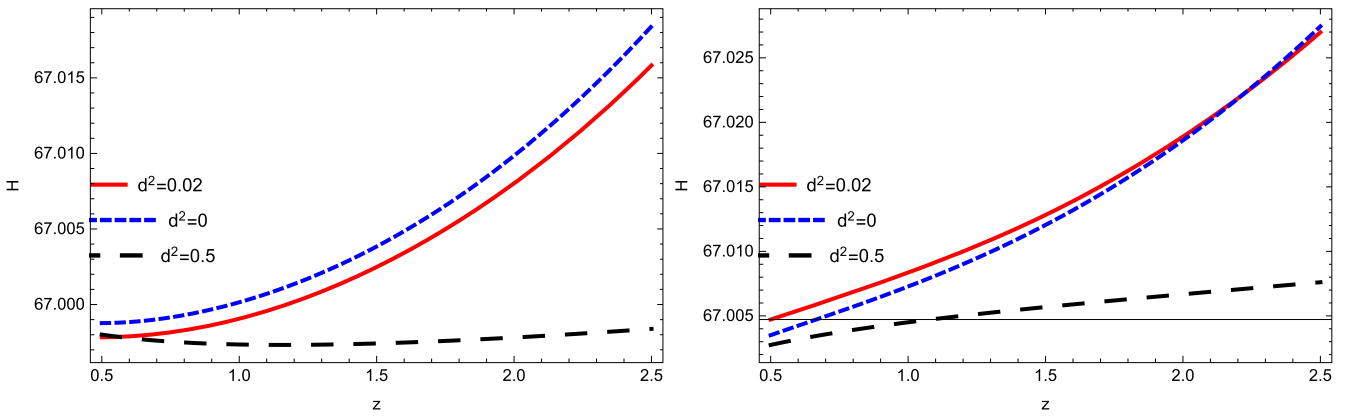


Figure 3. Plot of H versus z for $k = 1$ and $k = -1$ respectively.

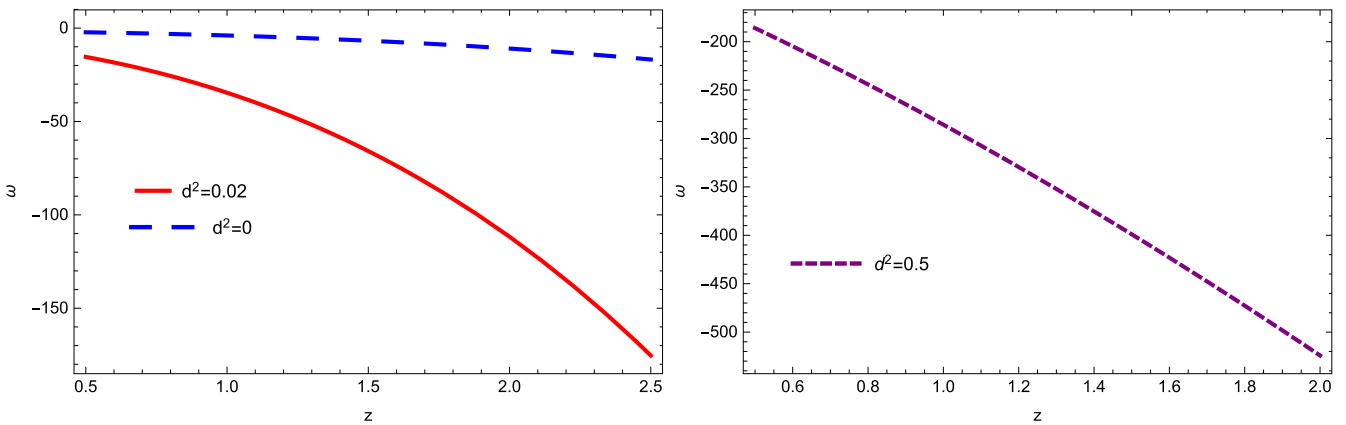


Figure 4. Plot of ω versus z for $k = 1$.

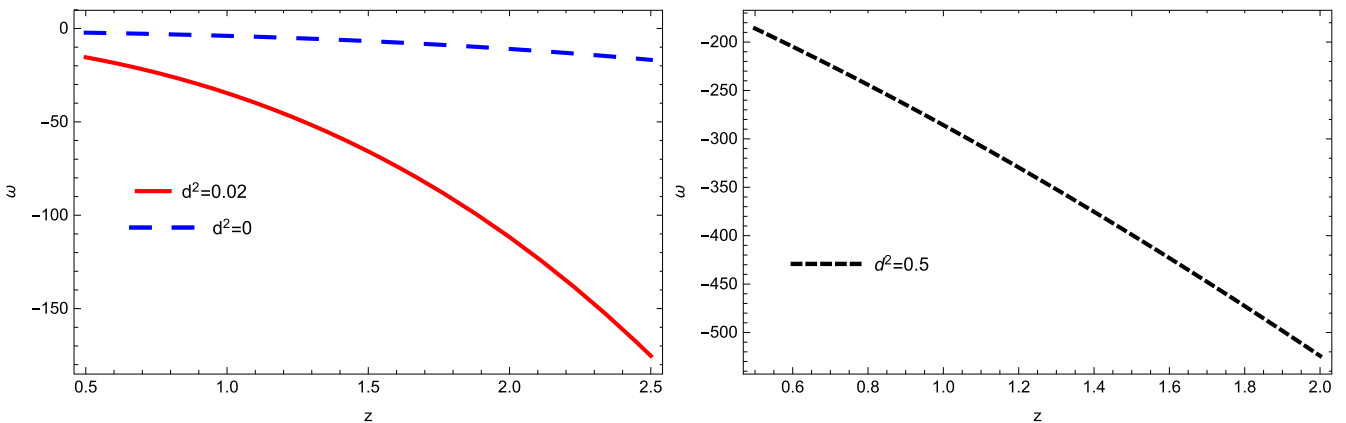


Figure 5. Plot of ω versus z for $k = -1$.

Also, we obtain the following form of Hubble parameter as by using equations (2.10)

$$H = \frac{\alpha}{\beta}, \tag{2.12}$$

here Hubble parameter is constant. We numerically plot the Hubble parameter against the redshift parameter z for three different values of interacting parameter $d^2 = 0.02, 0.0, 0.5$.

We consider $H(0.1) = 67$ as initial guess and the values of other parameters are $H_0 = 70, u = 2, \alpha = 25.65, \beta = -0.37, \Omega_{m0} = 0.27$ and $\varrho_{m0} = 0.73$. We observe the plot of H , which shows the increasing behavior for the two different values of $\kappa = -1, 1$ as shown in figure 3. The trajectories of H exhibits smooth transition from decelerated to accelerated epoch. These observation shows the consistent behavior with the current days observations.

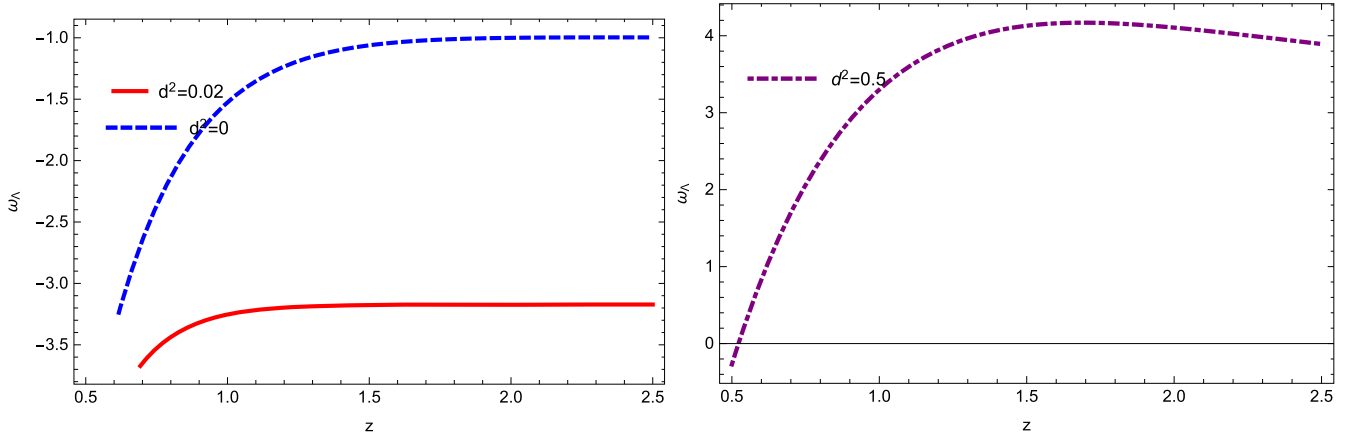


Figure 6. Plot of ω versus z when H is constant.

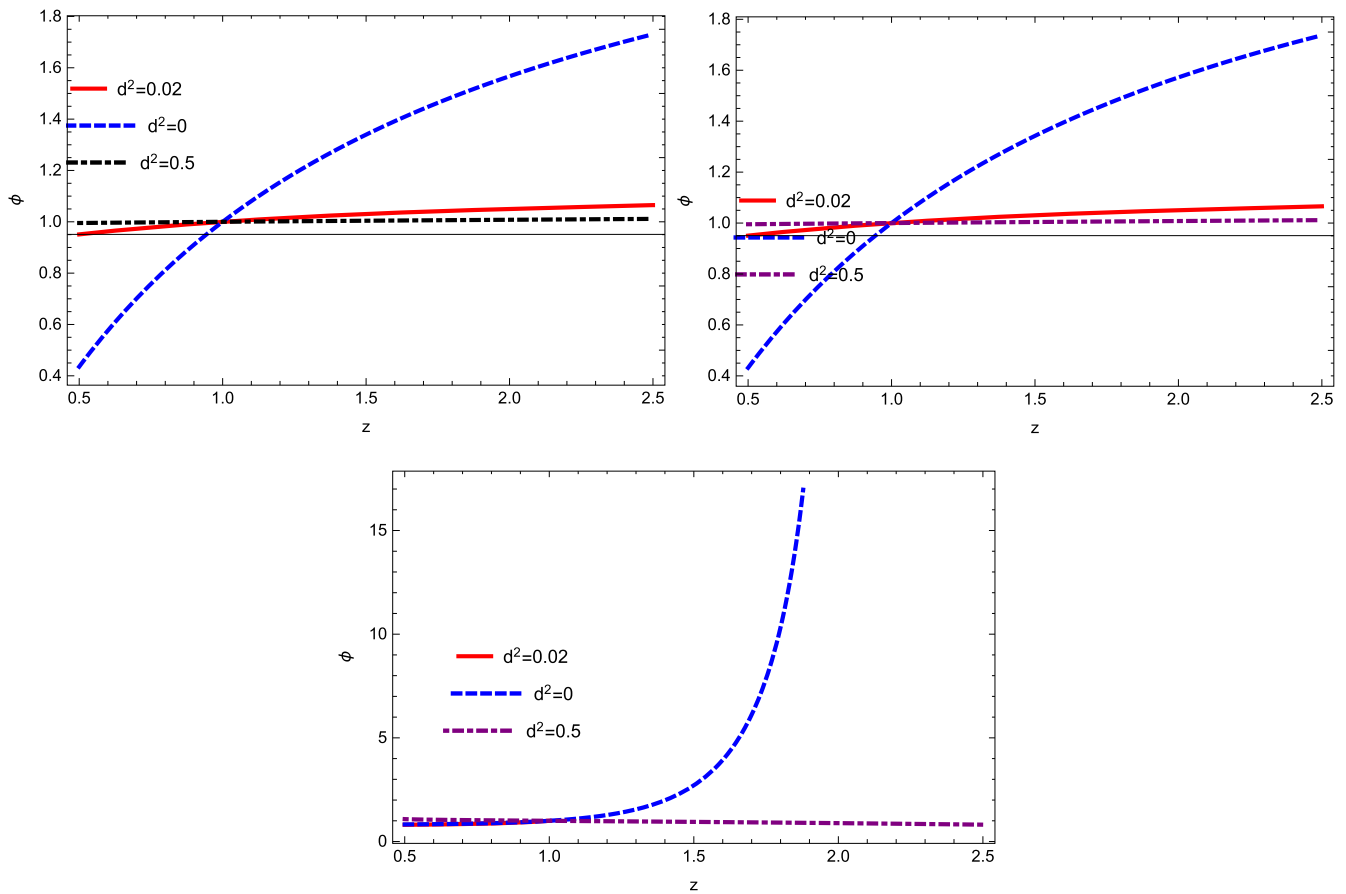


Figure 7. Plot of ϕ versus z for $k = 1$ (left) and $k = -1$ (right) respectively and plot of ϕ versus z when H is constant for quintessence scalar field model.

With the help of equations (2.5) and (2.6), we obtain the EoS parameter for interacting GGPDE

$$\begin{aligned} \omega_\Lambda = & -1 - 3a^{3(d^2-1)}d^2H\rho_{m0} - \gamma(\alpha + 2\beta H) \\ & \times (-2\kappa a^{-2} + 3a^{3(d^2-1)} \times (d^2 - 1)H^2\Omega_{m0}) \\ & \times (3H^2(\alpha + \beta H)(2(\alpha + \beta H) \\ & - (\alpha + 2\beta \times H)\gamma\Omega_\Lambda(\alpha + \beta H)^{-1}))^{-1}. \end{aligned} \quad (2.13)$$

Here, we get the following form of EoS parameter by using equations (2.5) and (2.10)

$$\begin{aligned} \omega_\Lambda = & (-2(\alpha(1+z)d^2 + \beta + (-1-z)\alpha) \\ & \times c_1(d^2 - 1)e^{\frac{-3a(d^2-1)z}{b}} + \left(d^2 \times \left(\frac{-\alpha^2}{\beta}\right)(2 + \gamma + \gamma^2) \right. \\ & \left. - 2d^2 + 2)\beta)(2\beta d^2 - 2\beta)^{-1} \end{aligned} \quad (2.14)$$

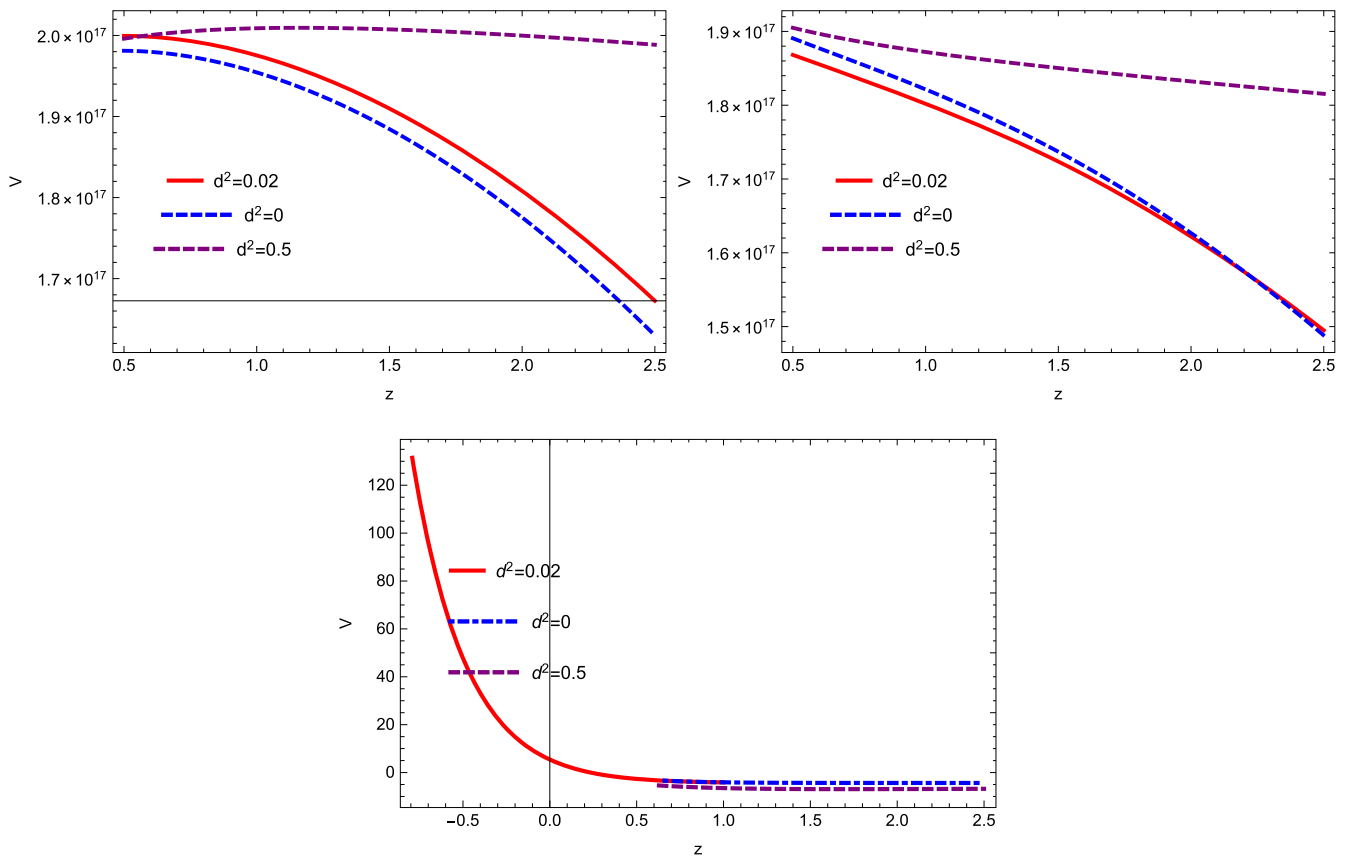


Figure 8. Plot of V versus z for $k = 1$ and $k = -1$ respectively and plot of V versus z when H is constant for quintessence scalar field model.

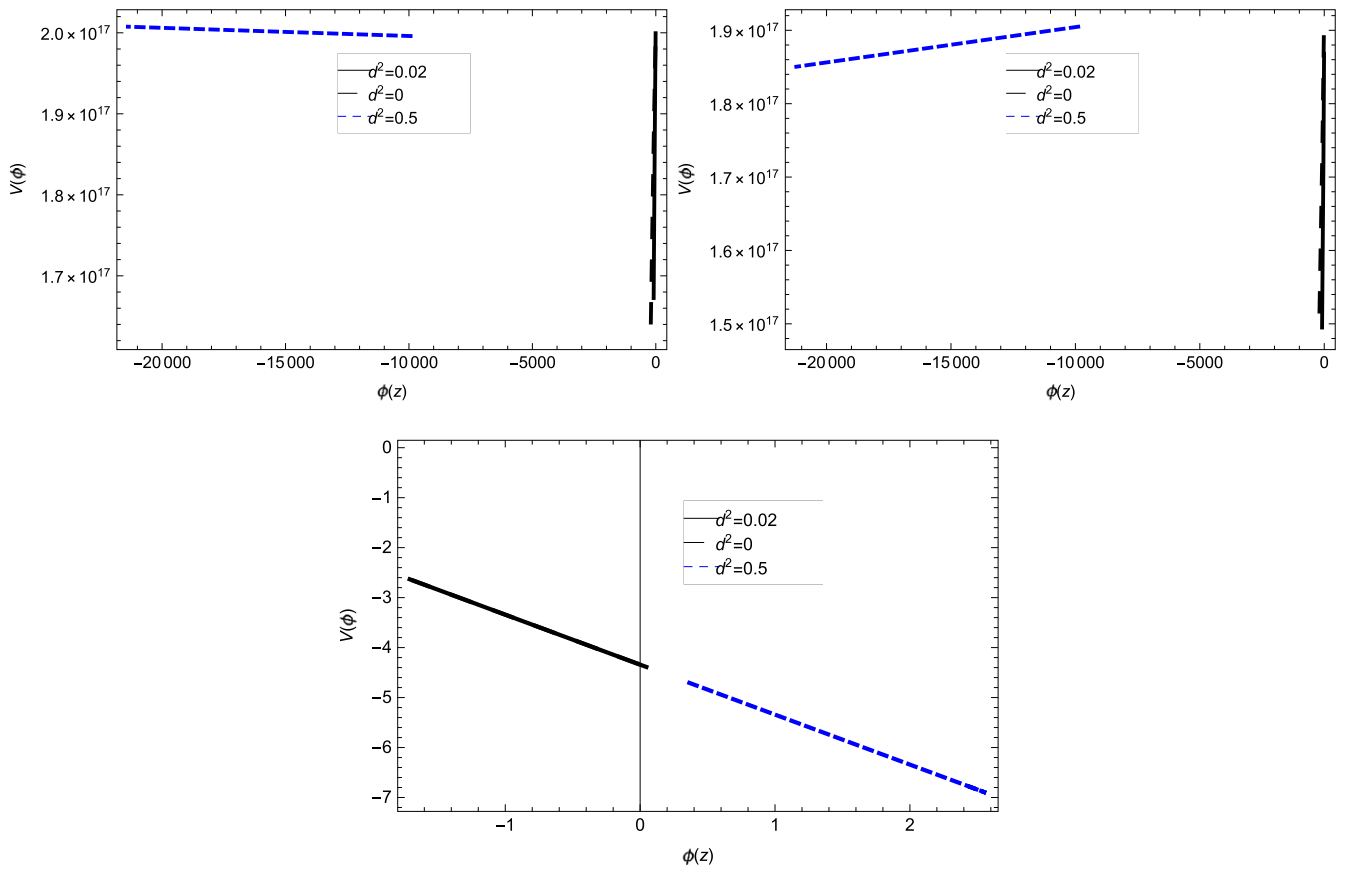


Figure 9. Plot of $\phi(z)$ versus $V(\phi)$ for $k = 1$ and $k = -1$ and when H is constant for quintessence scalar field model.

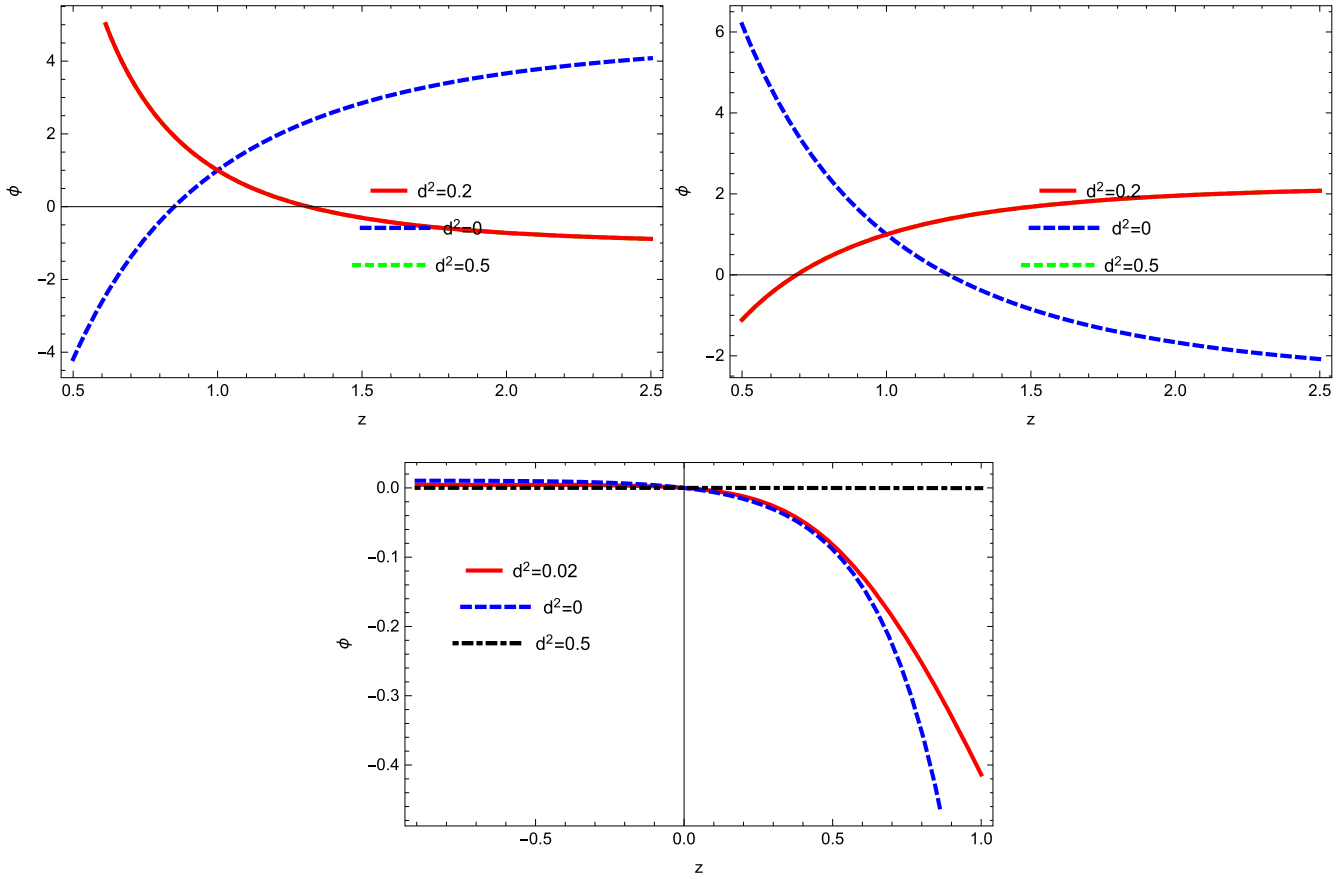


Figure 10. Plot of ϕ versus z for $k = 1$ and $k = -1$ respectively and when H is constant for tachyon scalar field model.

EoS parameter characterizes the cosmos into different eras such as radiation, matter and DE dominated era for $\omega = \frac{1}{3}$, $\omega = 0$ and $\omega = -1$. DE era is also divided into two phases as quintessence ($-1 < \omega \leq \frac{-1}{3}$) and phantom ($\omega < -1$) phases.

For the statefinder parameter

$$r = \frac{\ddot{a}}{aH^3}, s = \frac{r - 1}{3(q - \frac{1}{2})}, \tag{2.15}$$

also

$$r = 2q^2 + q - \frac{\dot{q}}{H}. \tag{2.16}$$

where q is the deceleration parameter. For ϱ_{m1} , the trajectories of $r - s$ parameter corresponds to Λ CDM for all values of interacting parameter [32] but for ϱ_{m2} it exhibits constant behavior.

In figures 4 and 5, the EoS parameter tends to lie in DE dominated era. For $k = 1$ and $k = -1$, the plot of EoS parameter is in phantom phase. Figure 6 shows that the trajectories of EoS parameter lie in quintessence phase and then goes toward phantom region for $d^2 = 0.02, 0.0$ when H is constant. For $d^2 = 0.5$, the plot of EoS parameter shows increasing behavior and tends to lie radiation dominated era.

3. Reconstruction of GGPDE scalar field models

In this portion, we check the correspondence of interacting GGPDE with tachyon, quintessence, K-essence and dilaton field models in non-flat universe.

3.1. GGPDE quintessence model

EoS is considered to be time dependent instead of constant then the fine tuning problem may be resolved which implies the proposal of quintessence scalar field model. This model possesses the ability to explain the cosmic acceleration by generating negative pressure where potential dominates the kinetic term [31].

Quintessence scalar field model is used to explain the acceleration of cosmos from negative pressure when potential is dominated by kinetic term. The potential is useful to analyze the early inflation and the late time acceleration. The pressure and energy density of the quintessence scalar field model are given as [39]

$$p_q = \frac{1}{2}\dot{\phi}^2 - V(\phi), \varrho_q = \frac{1}{2}\dot{\phi}^2 + V(\phi), \tag{3.1}$$

here $\dot{\phi}^2$ and $V(\phi)$ is known as kinetic energy and scalar potential, respectively. The EoS parameter of this model is

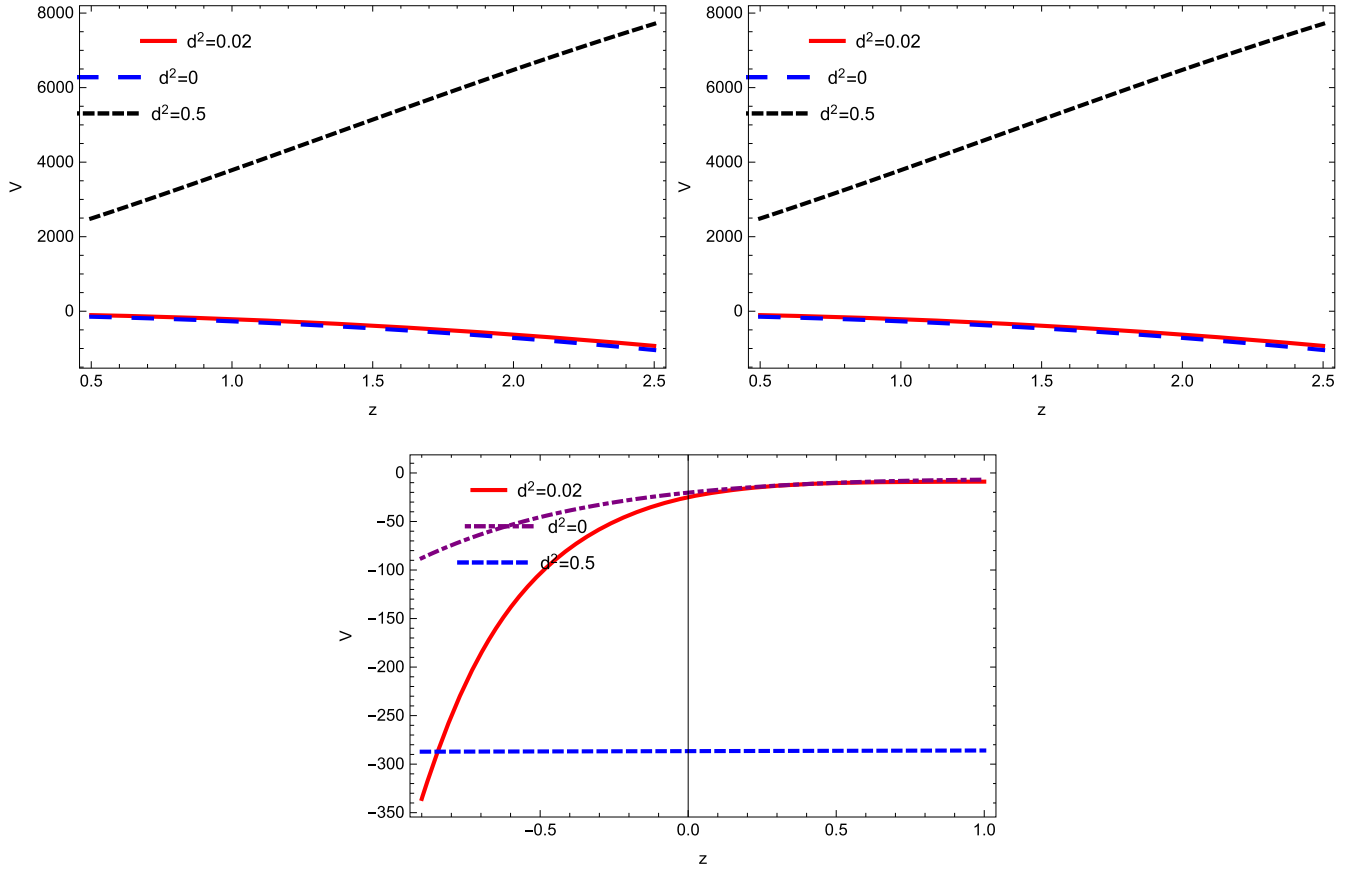


Figure 11. Plot of V versus z for $k = 1$ and $k = -1$ respectively and when H is constant for tachyon scalar field model.

defined as

$$\omega_q = \frac{\dot{\phi}^2 - 2V(\phi)}{\dot{\phi}^2 + 2V(\phi)}. \quad (3.2)$$

To establish the correspondence between the GGPDE and quintessence scalar field model, we put $\varrho_q = \varrho_\Lambda$ and $p_q = p_\Lambda$. Equation (3.2) gives

$$\begin{aligned} \dot{\phi} = & (-3a^{3(d^2-1)}d^2H\varrho_{m0}(\alpha H + \beta H^2)^\gamma \\ & - \gamma(\alpha H + \beta H^2)^\gamma(\alpha + 2\beta \times H)(-2\kappa a^{-2} + 3a^{3(d^2-1)} \\ & \times (d^2 - 1)H^2\Omega_{m0})(3H^2(\alpha + \beta H)(2(\alpha \\ & + \beta H) - (\alpha + 2\beta H)\gamma\Omega_\Lambda(\alpha + \beta H)^{-1}))^{-\frac{1}{2}}. \end{aligned} \quad (3.3)$$

The quintessence potential is given as

$$\begin{aligned} V(\phi) = & (\alpha H + \beta H^2)^\gamma + \frac{3}{2}a^{3(d^2-1)} \\ & \times d^2H\varrho_{m0}(\alpha H + \beta H^2)^\gamma + (\gamma(\alpha H + \beta H^2)^\gamma \\ & \times (\alpha + 2\beta H)(-2\kappa a^{-2} + 3a^{3(d^2-1)}(d^2 - 1)H^2\Omega_{m0})) \\ & \times (6H^2 \times (\alpha + \beta H)(2(\alpha + \beta H) - (\alpha + 2\beta H)\gamma \\ & \times \Omega_\Lambda(\alpha + \beta H)^{-1}))^{-1}. \end{aligned} \quad (3.4)$$

Similar expressions can be obtained for ϱ_{m2} .

The studies of scalar potentials and kinetic energies play a significant role to understand the cosmic expansion. The field ϕ

exhibits negative behavior and potential dominates over the kinetic energy ($\frac{\dot{\phi}^2}{2} < V(\phi)$) for accelerated expansion. For decelerated expansion, negative potential follows kinetic energy ($\frac{\dot{\phi}^2}{2} > V(\phi)$). We plot scalar field ϕ numerically versus redshift parameter z by taking $\phi(1) = 1$ as initial guess, while keeping the same values of other constant parameters. For quintessence scalar field model, figure 7 shows the increasing behavior with the passage of time for $d^2 = 0.02$ and shows a smooth transition for $d^2 = 0$ and 0.5 . The plot of potential V against z is shown in figure 8, indicating the increasing behavior. According to the condition, the large value of quintessence potential V shows the accelerated expansion of the Universe. The dominated potential over kinetic energy leads toward accelerated universe. Figure 9 shows the accelerated expansion, as the kinetic energy evolves the negative behavior and the potential dominates over the kinetic energy for $k = 1$ and $k = -1$ respectively. In the lower panel, the field kinetic energy shows transition from negative to positive and potential exhibits negative behavior showing decelerated expansion as H is constant

3.2. GGPDE tachyon model

The tachyon model has been proposed to discuss the structure of DE and it is an interesting fact that a rolling tachyon smoothly incorporates the values of EoS parameter between -1 to 0 . Also, it is the best applicant for high energy inflation.

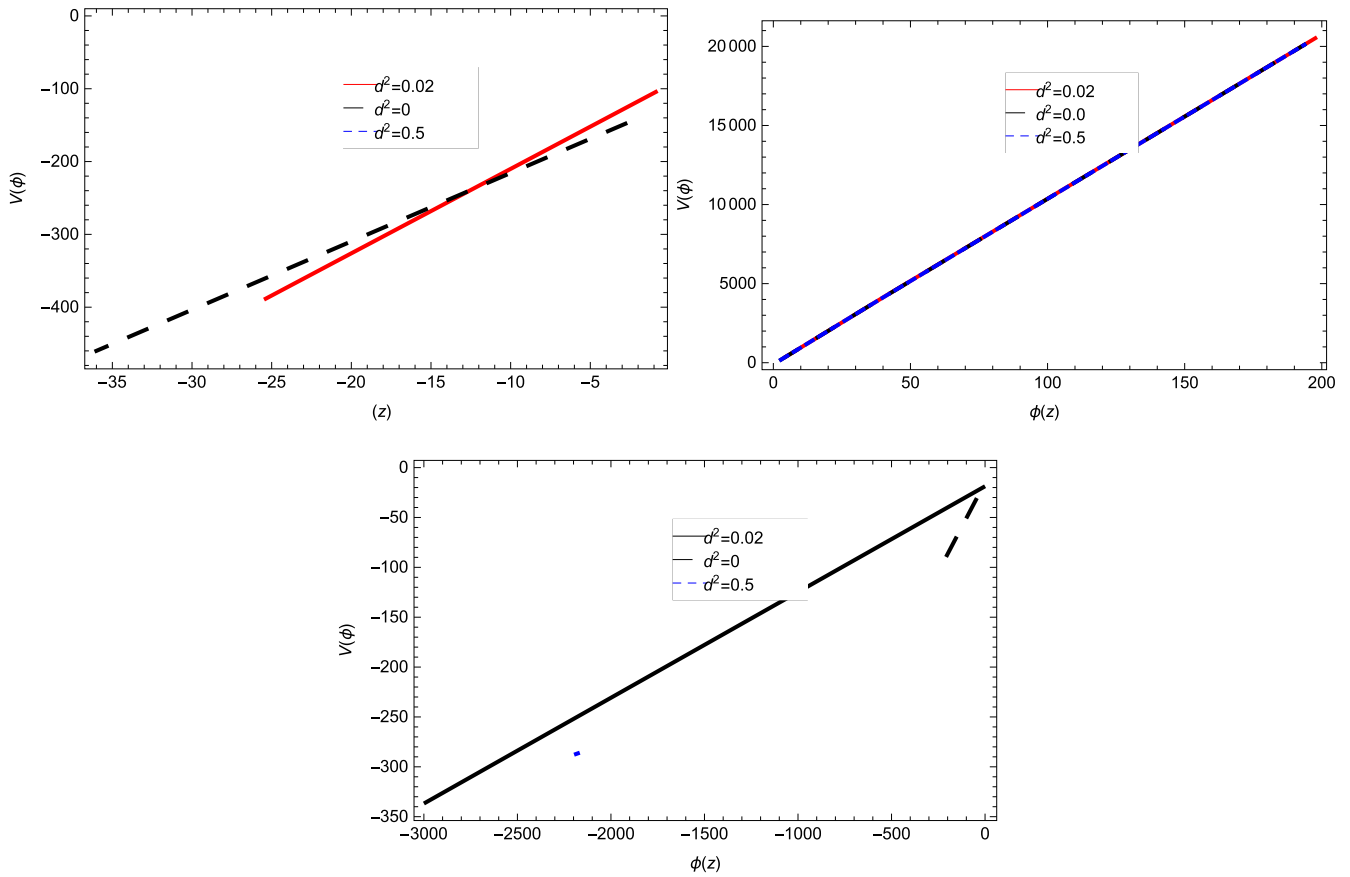


Figure 12. Plot of $\phi(z)$ versus $V(\phi)$ for $k = 1$ and $k = -1$ and when H is constant for tachyon scalar field model.

The Lagrangian of this model is defined as [39]

$$L = -V(\phi)\sqrt{1 + \partial_u\phi\partial^u\phi}, \tag{3.5}$$

where $V(\phi)$ is termed as tachyon potential. The energy and pressure of current model is given as

$$\rho_t = \frac{V(\phi)}{\sqrt{1 - \dot{\phi}^2}}, p_t = -V(\phi)\sqrt{1 - \dot{\phi}^2}. \tag{3.6}$$

The EoS parameter is interpret as

$$\omega_t = \dot{\phi}^2 - 1. \tag{3.7}$$

To obtain the correspondence between GGPDE and tachyon model, we set $\varrho_t = \varrho_\Lambda$ and $p_t = p_\Lambda$ which gives

$$\begin{aligned} \dot{\phi}^2 = & -3a^{3(d^2-1)}d^2H\varrho_{m0} - \gamma(\alpha + 2\beta H) \\ & \times (-2\kappa a^{-2} + 3a^{3(d^2-1)} \times (d^2 - 1)H^2\Omega_{m0}) \\ & \times (3H^2(\alpha + \beta H)(2(\alpha + \beta H) \\ & - (\alpha + 2\beta \times H)\gamma\Omega_\Lambda(\alpha + \beta H)^{-1}))^{-1}. \end{aligned} \tag{3.8}$$

The tachyon potential is given as

$$\begin{aligned} V(\phi) = & -(\alpha + \beta H^2)^\gamma(1 + 3a^{3(d^2-1)}d^2H\varrho_{m0} \\ & + \gamma(\alpha + 2\beta H)(-2\kappa a^{-2} + 3a^{3(d^2-1)} \\ & \times (d^2 - 1)H^2\Omega_{m0})(3H^2(\alpha + \beta H)(2(\alpha + \beta H) \\ & - (\alpha + 2\beta \times H)\gamma\Omega_\Lambda(\alpha + \beta H)^{-1}))^{\frac{1}{2}}. \end{aligned} \tag{3.9}$$

Similar expressions can be obtained for ϱ_{m2} .

Here, we also plot numerically field ϕ against z with previous assumption. In figure 10, the plot of $\phi(z)$ decreases with the passage of time for non-flat universe for $d^2 = 0.02$ and 0.0 , while it show increasing behavior for $d^2 = 0.5$. Figure 11 shows the increasing behavior as z increases for both open and closed universe, whereas, the potential V shows decreasing behavior and become steeper later for constant value of Hubble parameter. Figure 12 shows that kinetic energy decreases with $V(z)$ increasing negatively but $V(z)$ decrease with increase in kinetic energy as universe tends to expand. It shows the decelerated expansion as the negative potential dominates over the kinetic energy for $k = 1$. For $k = -1$, both the kinetic energy and potential exhibits increasing behavior but potential dominates over the field kinetic energy showing the accelerated expansion. It is to be observed that the values of kinetic energy and potential are decreasing for constant value of Hubble parameter.

3.3. GGPDE K-essence scalar field model

K-essence model evolves the universe in the accelerated era as it is different from quintessence model. It is developed from the concept of K-inflation used to examine the early universe inflation at high energies [40].

This was used for DE purpose and was further extended to get more general form of Lagrangian having K-essence

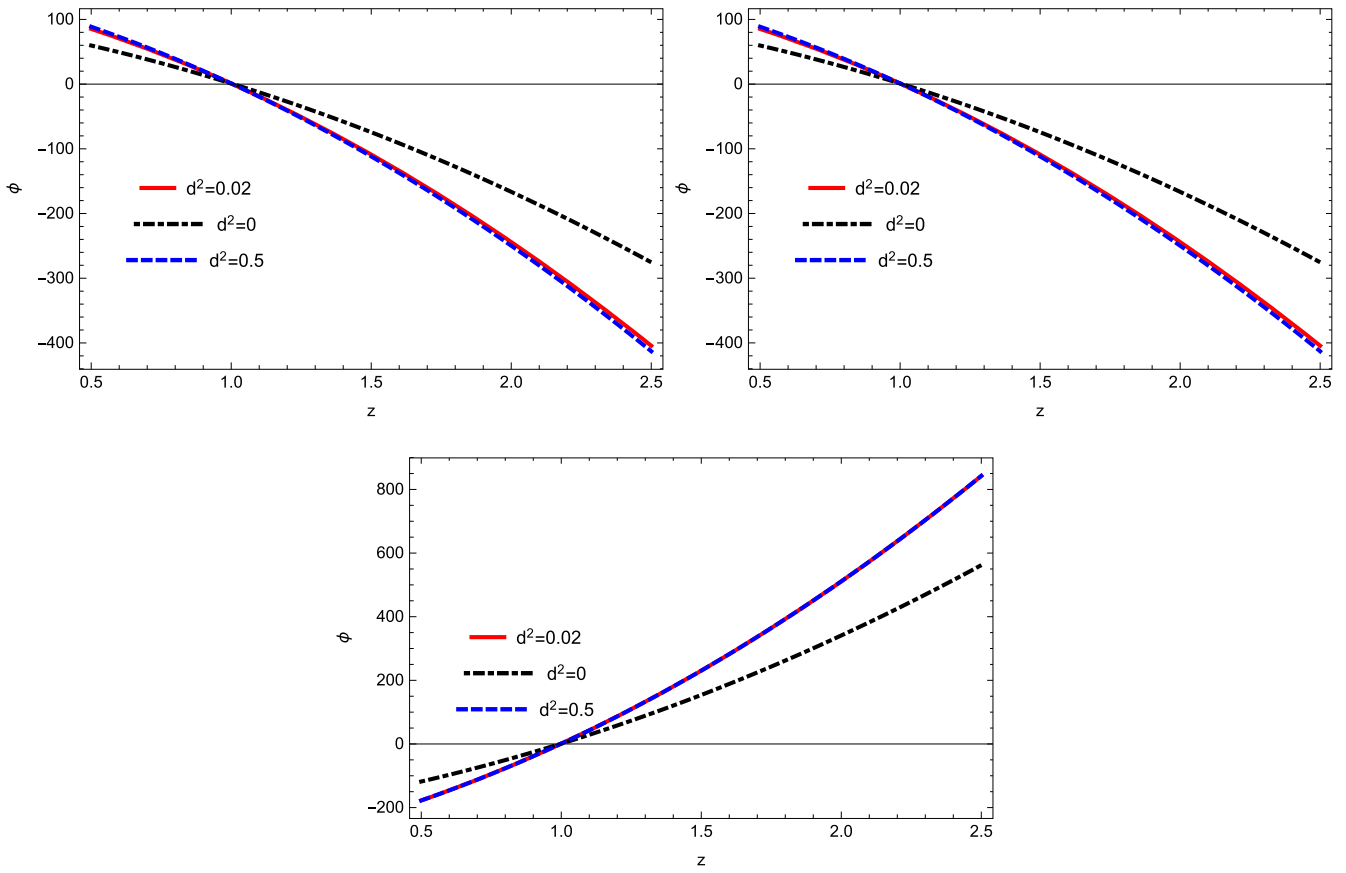


Figure 13. Plot of ϕ versus z for $k = 1$ and $k = -1$ and when H is constant for K-essence model.

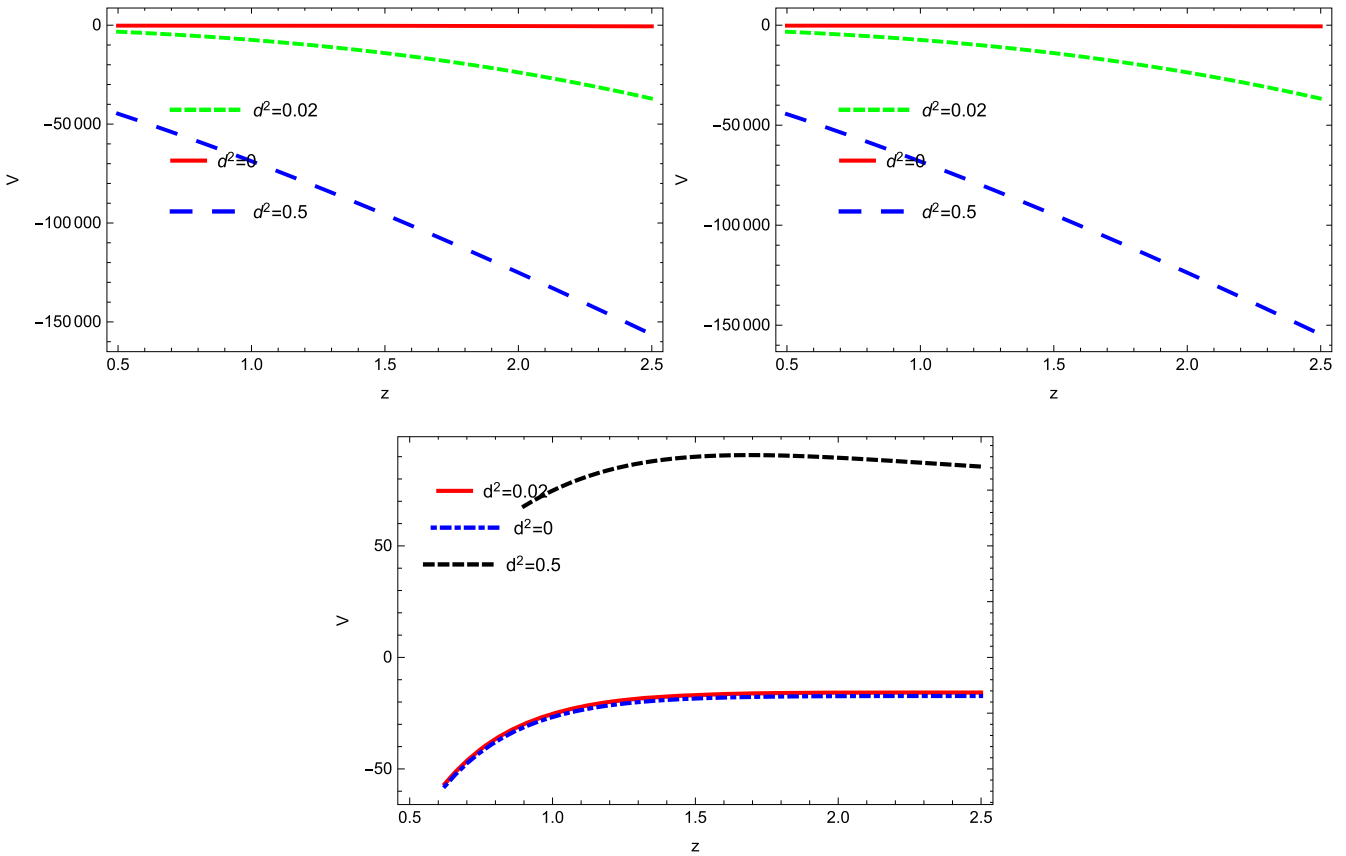


Figure 14. Plot of V versus z for $k = 1$ and $k = -1$ and when H is constant for K-essence model.

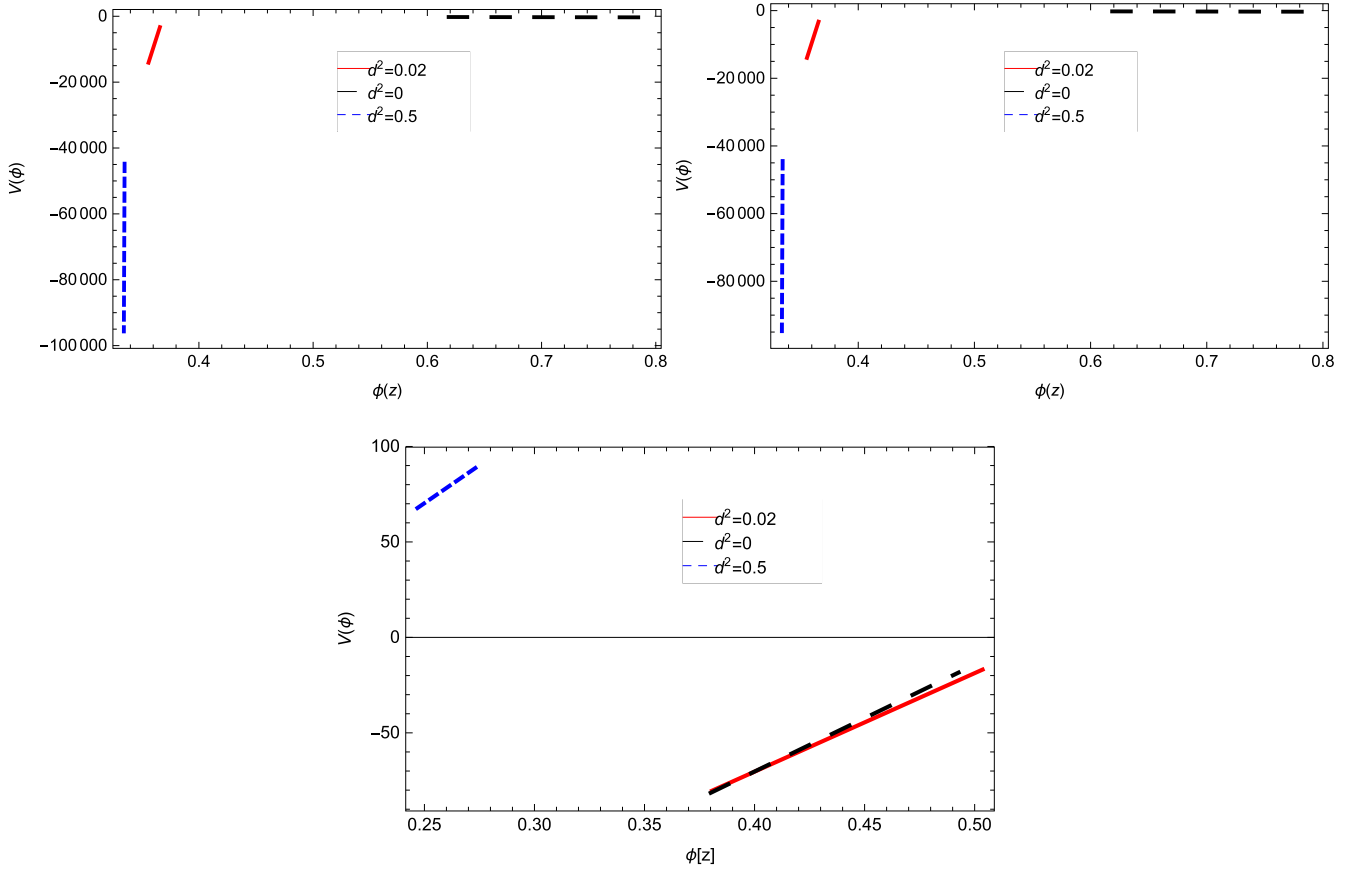


Figure 15. Plot of $\phi(z)$ versus $V(\phi)$ for $k = 1$ and $k = -1$ and when H is constant for K-essence model.

[41, 42]. The generalized scalar field action is defined as [43]

$$S = \int d^4x \sqrt{-gp(\phi, \chi)}, \quad (3.10)$$

here $p(\phi, \chi)$ define the pressure density as a function of ϕ and $\chi = \frac{1}{2}\dot{\phi}^2$. The K-essence model have the energy density and scalar field pressure as

$$\rho_k = V(\phi)(-\chi + 3\chi^2), \quad p_k = V(\phi)(-\chi + \chi^2),$$

where $V(\phi)$ is the scalar potential of K-essence model. The EoS of K-essence is given as

$$\omega_k = \frac{1 - \chi}{1 - 3\chi}. \quad (3.11)$$

For the correspondence between GGPDE and K-essence model, we obtain

$$\begin{aligned} \chi = & (-2 - 3a^{3(d^2-1)}d^2H\varrho_{m0} - \gamma(\alpha + 2\beta H) \\ & \times (-2\kappa a^{-2} + 3a^{3(d^2-1)} \times (d^2 - 1)H^2\Omega_{m0}) \\ & \times (3H^2(\alpha + \beta H)(2(\alpha + \beta H) - (\alpha + 2\beta H)\gamma\Omega_\Lambda \\ & \times (\alpha + \beta H)^{-1}))^{-1}(-4 - 9a^{3(d^2-1)} \\ & \times d^2H\varrho_{m0} - \gamma(\alpha + 2\beta H)(-2\kappa \times a^{-2} + 3a^{3(d^2-1)} \\ & \times (d^2 - 1)H^2\Omega_{m0})(3H^2(\alpha + \beta H)(2(\alpha + \beta H) \\ & - (\alpha + 2\beta H)\gamma\Omega_\Lambda(\alpha + \beta H)^{-1}))^{-1}, \end{aligned} \quad (3.12)$$

where $\chi = \frac{\dot{\phi}}{2}$.

$$V(\phi) = \frac{(\alpha H + \beta H^2)^\gamma (3\omega_k - 1)^2}{-2(\omega_k - 1)}. \quad (3.13)$$

Similar expressions can be obtained for ϱ_{m2} .

Figure 13 shows that the scalar field $\phi(z)$ decrease with time for open as well as closed universe, where it shows increasing behavior when H is constant. The K-essence potential $V(z)$ decreases with passage of time as shown in figure 14 for all the cases. The kinetic energy χ lies in required interval $(\frac{1}{3}, \frac{2}{3})$ from early epoch to later epoch as in figure 15. EoS parameter shows that accelerated expansion lies in this interval, for $\chi < \frac{1}{2}$, it tends to lie in phantom DE phase. For $k = 1$ and $k = -1$, the plot potential $V(z)$ exhibits negatively increasing behavior which shows the Universe is in accelerating era. For $d^2 = 0.02$ and 0.0 , the potential shows negative behavior and kinetic energy shows increasing behavior exhibits decelerated expansion as H is constant. Whereas for $d^2 = 0.5$, the potential dominated over the kinetic energy confirming the accelerated expansion of the Universe.

3.4. GGPDE dilaton field

The Lagrangian of dilaton field is termed as pressure and energy density [40]

$$p_d = -\chi + b_1 e^{b_2 \phi} \chi^2, \quad \rho_d = -\chi + 3b_1 e^{b_2 \phi} \chi^2, \quad (3.14)$$

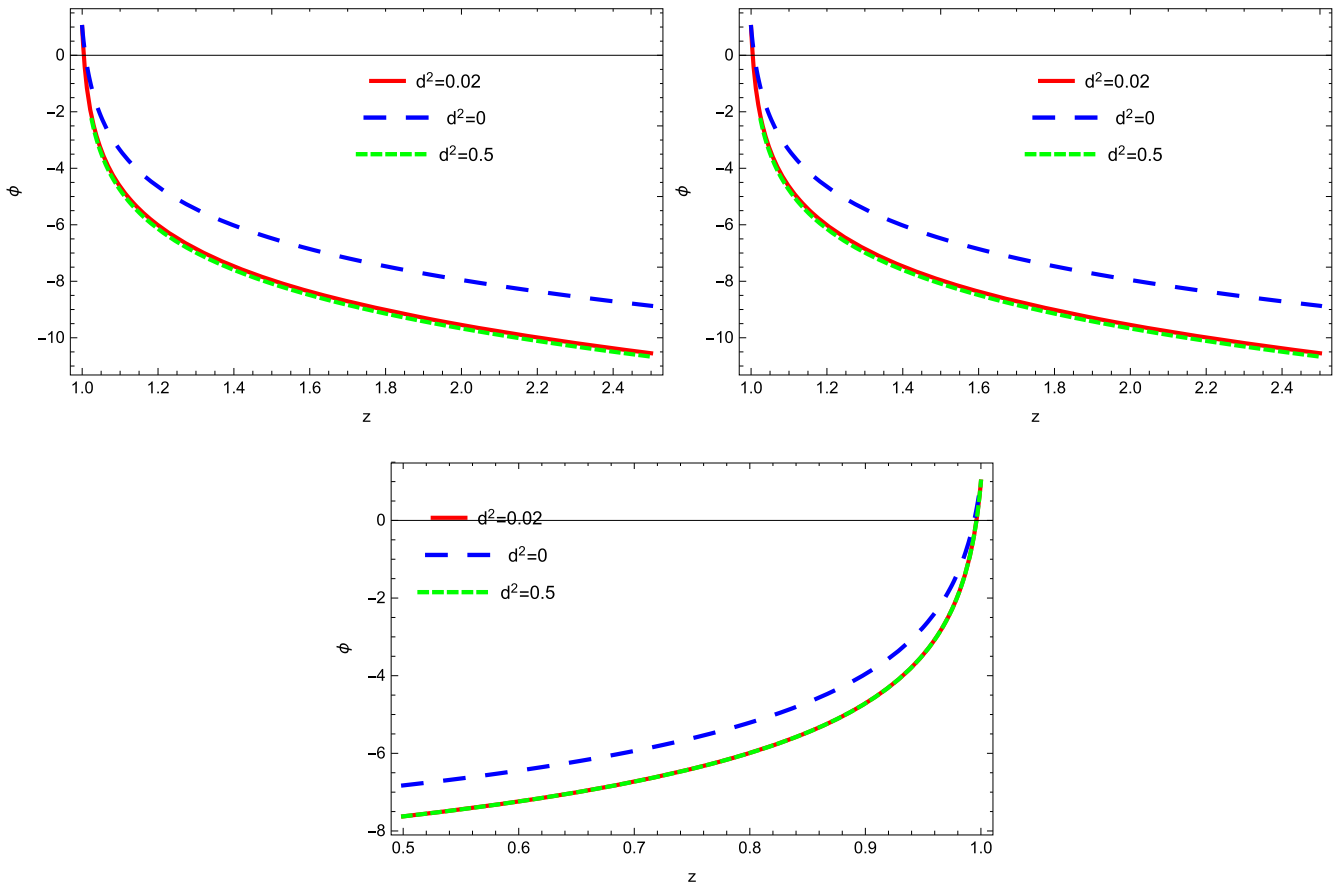


Figure 16. Plot of ϕ versus z for $k = 1$ and $k = -1$ and when H is constant for dilaton model.

where b_1 and b_2 are positive constants. The EoS is given as

$$\omega_d = \frac{-1 + b_1 e^{b_2 \phi} \chi}{-1 + 3b_1 e^{b_2 \phi} \chi} \quad (3.15)$$

By putting $\varrho_d = \varrho_\Lambda$ and $p_d = p_\Lambda$, we get

$$\begin{aligned} e^{b_2 \phi} \chi &= \frac{1}{b_1} (-1 - 3a^{3(d^2-1)} d^2 H \varrho_{m0}) \\ &- \gamma (\alpha + 2\beta H) (-2\kappa a^{-2} + 3 \times a^{3(d^2-1)} (d^2 - 1) H^2 \Omega_{m0}) \\ &\times (3H^2 (\alpha + \beta H) (2(\alpha + \beta H) - (\alpha + 2\beta H) \gamma) \\ &\times \Omega_\Lambda (\alpha + \beta H)^{-1})^{-1} (-4 - 9a^{3(d^2-1)} d^2 H \varrho_{m0}) \\ &- \gamma (\alpha + 2\beta H) (-2\kappa a^{-2} + 3a^{3(d^2-1)} (d^2 - 1) H^2 \Omega_{m0}) \\ &\times \left(3H^2 \times (\alpha + \beta H) \left(2(\alpha + \beta H) - \frac{(\alpha + 2\beta H) \gamma \Omega_\Lambda}{(\alpha + \beta H)} \right)^{-1} \right)^{-1} \end{aligned} \quad (3.16)$$

$$\begin{aligned} \phi(a) &= \frac{2}{b_2} \int \ln \left[\frac{1}{b_1} (-1 - 3a^{3(d^2-1)} d^2 H \varrho_{m0}) \right. \\ &- \gamma (\alpha + 2\beta H) (-2\kappa \times a^{-2} + 3a^{3(d^2-1)} (d^2 - 1) H^2 \Omega_{m0}) \\ &\times (3H^2 (\alpha + \beta H) (2(\alpha + \beta H) - (\alpha + 2\beta H) \gamma) \\ &\times \Omega_\Lambda (\alpha + \beta H)^{-1})^{-1} (-4 - 9a^{3(d^2-1)} d^2 H \varrho_{m0}) \\ &- \gamma (\alpha + 2\beta H) (-2\kappa a^{-2} + 3a^{3(d^2-1)} (d^2 - 1) H^2 \Omega_{m0}) (3H^2 \\ &\times (\alpha + \beta H) \left(2(\alpha + \beta H) - \frac{(\alpha + 2\beta H) \gamma \Omega_\Lambda}{(\alpha + \beta H)} \right)^{-1} \left. \right]^{\frac{1}{2}} \end{aligned} \quad (3.17)$$

Similar expressions can be obtained for ϱ_{m2} .

The plot of figure 16 shows the decreasing behavior with time as $\phi(z)$ decreases with the passage of time. The EoS parameter bounds $e^{b_2 \phi} \chi$ to lie in interval $(\frac{20}{3}, \frac{40}{3})$ for accelerated expansion. Figure 17 show that the increase in $e^{b_2 \phi} \chi$ with increase in z as it tends to lie in appropriate interval.

4. Final remarks

In this work, we have considered the interacting GGPDE model in the background of non-flat FRW universe. We have constructed two cosmological parameters in order to check the behavior of current model i.e. Hubble and EoS parameters. We have discussed the current model with suitable choice of interacting parameter i.e. $d^2 = 0.02, 0.0$ and 0.5 by considering two forms of interaction terms Also, we have observed the correspondence of current model with some scalar field models having quintessential behavior with dilaton, K-essence, tachyon and quintessence scalar field models. We have also checked graphically the dynamical DE models having scalar field and their corresponding potentials through interacting parameter. We have discussed the quintessence, phantom, K-essence and dilaton scalar field models with the suitable choice of interacting parameters. The concluding remarks for non-flat universe is given as

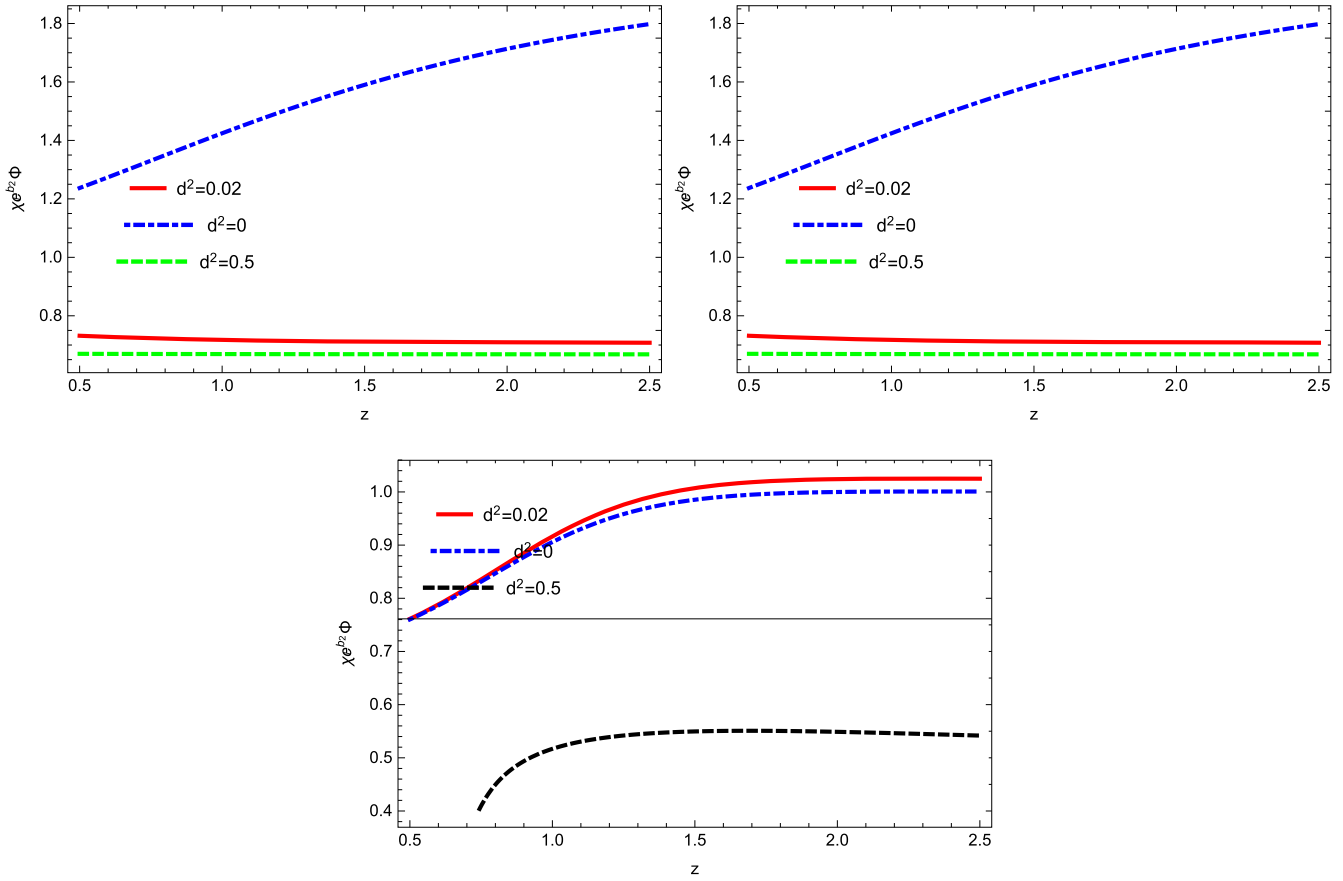


Figure 17. Plot of $e^{b_2\phi}\chi$ versus z for $k = 1$ and $k = -1$ and when H is constant for dilaton model.

- For closed universe, plot of Ω_{m1} reveals the consistent behavior with Plancks 2018 while for open universe it exhibits inconsistent behavior. Ω_{m2} also shows inconsistent behavior with recent observations of Plancks for different values of interacting parameter. Observation of Plancks 2018 [44] introduced the different values of Ω_m at 68% percent limit

$$\Omega_m = 0.289^{+0.026}_{-0.033} \quad (\text{EE} + \text{lowE}),$$

$$\Omega_m = 0.3153 \pm 0.0073$$

(Planck TT, TE, EE + lowE + lensing),

$$\Omega_m = 0.3111 \pm 0.0056$$

(Planck TT, TE, EE + lowE + lensing + BAO).

It is worthwhile to mention here that the fractional densities of matter (Ω_m) shows compatible behavior for different values of interacting parameter.

- The DE fractional density shows consistent behavior with Plancks 2018 for closed universe whereas it does not show consistent behavior for open universe. Recent observations of Planck 2018 proposed different values of Ω_Λ at 68% given by [44]

$$\Omega_\Lambda = 0.711^{+0.033}_{-0.026} \quad (\text{EE} + \text{lowE}),$$

$$\Omega_\Lambda = 0.6847 \pm 0.0073$$

(Planck TT, TE, EE + lowE + lensing),

$$\Omega_\Lambda = 0.6889 \pm 0.0056$$

(Planck TT, TE, EE + lowE + lensing + BAO).

- The plot of Hubble parameter is showing the increasing behavior as the Universe is in accelerating phase which have a consistent behavior with the current days observations. Plancks 2018 [44] also proposed different values of Hubble constant as

$$H_0 = 69.9 \pm 2.7 \quad (\text{EE} + \text{lowE}),$$

$$H_0 = 67.36 \pm 0.54$$

(Planck TT, TE, EE + lowE + lensing),

$$H_0 = 67.66 \pm 0.42$$

(Planck TT, TE, EE + lowE + lensing + BAO).

It is valuable to mention here that our current model shows the compatible behavior with the current days observations.

- The EoS parameter exhibits that the current model tends to lie in DE dominated era as for the ω_Λ lies in phantom phase for non-flat universe. For the constant value of Hubble parameter, the EoS parameter tends to lie in quintessence region at first and then move toward phantom region later.
- For quintessence scalar field model, ϕ exhibits increasing behavior with time while the quintessence potential shows the positive behavior. The comparison plot of $\phi(z)$ and $V(\phi)$ indicates the accelerated expansion as $V(\phi) > \phi(z)$.

- For tachyon model, ϕ shows the decreasing behavior while potential increases negatively with the passage of time. For accelerated expansion of universe the $V(\phi)$ decreases as $\phi(z)$ increases but it shows the decelerated expansion as the potential dominated over the kinetic energy.
- For K-essence model, we have plotted $\phi(z)$ and $V(\phi)$ for K-essence model, which exhibits the decreasing behavior. The χ tends to lie in required interval, which shows the expansion of universe, while the $V(\phi)$ increases with decrease in $\phi(z)$ as it shows the decelerated expansion.
- For dilaton model, $\phi(z)$ shows the decreasing behavior with time while $e^{b_2\phi}\chi$ exhibits the increasing behavior as it shows directly proportional with respect to time.

Abdul Jawad and Ujjal Denath [31] have discussed the interacting GGPDE in the framework of flat FRW universe. They have constructed the EoS parameter which shows the transition from quintessence region to phantom region at $z = -0.9$. At this negative value of redshift parameter, EoS parameter exhibits critical behavior, where it moves from one region to another. They have established the correspondence of GGPDE with different scalar field models. They have analyzed the dynamical scalar field models and their potentials in the presence of interacting parameters. For quintessence model, the potential increase as the Universe is in the phase of accelerated expansion. For tachyon model, they have observed that $\phi(z)$ decreases with increase in potential as universe expand. For K-essence scalar field model, the kinetic energy within the range of present observations, where the ω_k shows the accelerated expansion of the universe. For dilaton scalar field model, they have numerically plotted $e^{b_2\phi}\chi$ against z , which lies in the appropriate interval provides the accelerated expansion of the Universe.

We have discussed above the dynamical DE models with scalar field models and their corresponding potentials graphically in the presence of two interaction terms In order to check the consistent behavior, we have taken the suitable choice of interacting parameter d^2 . The Hubble parameter and quintessence scalar field model show the consistent behavior with the current days observations.

ORCID iDs

Wajiha Javed  <https://orcid.org/0000-0003-0276-0436>

References

- [1] Perlmutter S et al 1999 *Astrophys. J.* **517** 565
- [2] Caldwell R R and Doran M 2004 *Phys. Rev.* **69** 103517
- [3] Koivisto T and Mota D F 2006 *Phys. Rev. D* **73** 083502
- [4] Daniel S F 2008 *Phys. Rev. D* **77** 103513
- [5] Roos M 2003 *Introduction to Cosmology* (UK: Wiley)
- [6] Nojiri S and Odintsov S D 2011 Unified cosmic history in modified gravity, From F(R) theory to Lorentz non-invariant models *Phys. Rep.* **505** 59
- [7] Capozziello S and Faraoni V 2011 *Beyond Einstein Gravity* (New York: Springer)
- [8] Bamba K, Capozziello S, Nojiri S and Odintsov S D 2012 Dark energy cosmology: the equivalent description via different theoretical models and cosmography tests *Astrophys. Space Sci.* **342** 155
- [9] Li M, Li X D, Wang S and Wang Y 2013 *Universe* **1** 4
- [10] Nojiri S and Odintsov S D 2006 The new form of the equation of state for dark energy fluid and accelerating universe *Phys. Lett. B* **639** 144
- [11] Hsu S D H 2004 *Phys. Lett. B* **594** 13
- [12] Li M 2004 *Phys. Lett. B* **603** 1
- [13] Gao C J et al 2008 *Phys. Rev. D* **78** 024008
- [14] Wei H 2012 *Class. Quantum Grav.* **29** 175008
- [15] Cai R G et al 2012 *Phys. Rev. D* **86** 023511
- [16] Urban F R and Zhitnitsky A R 2009 *Phys. Rev. D* **80** 063
- [17] Das A 2002 *J. High Energy Phys.* **25** JHEP07(2002)065
- [18] Gasperini M et al 2002 *Phys. Rev. D* **65** 023508
- [19] Caldwell R R 2002 *Phys. Lett. B* **545** 23
- [20] Wei H, Cai R G and Zeng D F 2005 *Class. Quantum Grav.* **22** 16
- [21] Ratra B and Peebles P J E 1988 *Phys. Rev. D* **37** 3406
- [22] Wetterich C 1988 *Nucl. Phys. B* **302** 668
- [23] Zlatev I, Wang L and Steinhardt P J 1999 *Phys. Rev. Lett.* **82** 896
- [24] Steinhardt P J, Wang L and Zlatev I 1999 *Phys. Rev. D* **59** 123504
- Steinhardt P J, Wang L and Zlatev I 2005 *Phys. Rev. D* **72** 3189
- [25] Jamil M and Sheykhi A 2011 *Int. J. Theor. Phys.* **50** 625
- [26] Chattopadhyay S and Debnath U 2011 *Int. J. Theor. Phys.* **50** 315
- [27] Setare M R 2008 *Int. J. Mod. Phys. D* **12** 2219
- [28] Debnath U and Jamil M 2011 *Astrophys. Space Sci.* **335** 545
- [29] Jawad A and Debnath U 2014 *Adv. High Energy Phys.* **2014** 594781
- [30] Karami K and Khaledian M S 2011 *J. High Energy Phys.* **JHEP03(2011)086**
- [31] Jawad A, Debnath U and Batool F 2015 *Commun. Theor. Phys.* **64** 590–6
- [32] Jawad A 2014 *Eur. Phys. J. C* **74** 3214
- [33] Urban F R and Zhitnitsky A R 2009 *Phys. Rev. D* **80** 063001
- Urban F R and Zhitnitsky A R 2009 *J. Cosmol. Astropart. Phys.* **2009** JCAP09(2009)018
- [34] Granda L and Oliveros A 2009 *Phys. Lett. B* **671** 199
- [35] Granda L and Oliveros A 2008 *Phys. Lett. B* **669** 275
- [36] Karami K and Fehri J 2010 *Phys. Lett. B* **684** 61
- [37] Sheykhi A 2011 *Phys. Rev. D* **84** 107302
- [38] Sharif M and Jawad A 2012 *Eur. Phys. J. C* **72** 2097
- [39] Copeland E J, Sami M and Tsujikawa S 2006 *Int. J. Mod. Phys. D* **15** 1753
- [40] Piazza F and Tsujikawa S 2004 *J. Cosmol. Astropart. Phys.* **2004** JCAP07(2004)004
- [41] Chiba T, Okabe T and Yamaguchi M 2000 *Phys. Rev. D* **62** 023511
- [42] Armendariz-Picon C, Mukhanov V and Steinhardt P J 2001 *Phys. Rev. D* **63** 103510
- [43] Copeland E J, Sami M and Tsujikawa S 2006 *Int. J. Mod. Phys. D* **15** 1753
- [44] Aghanim N et al 2018 arXiv:1807.06209 [astro-ph.CO]